Applied Surface Science 422 (2017) 111–115

Contents lists available at ScienceDirect

Applied Surface Science

journal homepage: www.elsevier.com/locate/apsusc

Full Length Article

Depth-prediction method for direct laser-scribing processes

D. Canteli[a,b,*], J.J. García-Ballesteros[b], C. Molpeceres[b], J.J. Gandía[a], I. Torres[a,**]

[a] División de Energías Renovables, Energía Solar Fotovoltaica, CIEMAT, Avda. Complutense, 22, 28040, Madrid, Spain
[b] Centro Láser, Universidad Politécnica de Madrid, Alan Turing 1,, Madrid 28031, Spain

ARTICLE INFO

Article history:
Received 18 January 2017
Received in revised form 17 April 2017
Accepted 18 April 2017
Available online 21 April 2017

Keywords:
Laser processing
Transparent conductive oxides (TCO)

ABSTRACT

Many semiconductor technologies require the patterning of films to create features not easily achieved during growth or deposition. In the case of transparent conductive oxides (TCOs), this is typically realized through direct laser-scribing. Although there are models conceived to predict the depth of a scribe, the necessary parameters to obtain a given depth are usually found by trial and error. This is mostly due to the models usually being highly elaborated and dependent on difficult to measure variables.

In this paper we introduce a method for predicting the ablation depth in direct laser-scribing processes based on laser-processing parameters and convenient properties like the ablation threshold fluence and the laser penetration depth. In order to apply this method though, the materials must comply with two conditions: a) the material does not develop incubation with successive pulses and b) the ablation depth obtained at any position by a single pulse is determined by the fluence reaching that point. We present experimental data using nanosecond sources and a wavelength of 355 nm for TCOs Indium doped Tin Oxide and Aluminum doped Zinc Oxide that endorse the proposed method as a tool for predicting the ablated depth in laser scribes.

1. Introduction

Although laser grooving is an essential process in the semiconductor industry, there are not many studies aimed to predict the depth of the processes. Most of the models found in the literature that tackle this issue are for continuous wave laser sources scribing in metals [1–3] and composite materials [4–6] with only a relatively small number dedicated to pulsed laser processing [7–10]. On top of that, all of the mentioned models include complex processes such as heat fluxes, the apparition of plasma shielding, or the interaction between the laser light and melted material, making them difficult to implement.

In this paper we propose a simpler model that relates process parameters, pulse fluence and scanning velocity, to the depth of the obtained scribe for the case of pulsed laser sources. We have tested the proposed model in two different transparent conductive oxides (TCOs), Indium doped Tin Oxide (ITO) and Aluminum doped Zinc Oxide (AZO) and found the predictions to match very accurately the experimental results. Our choice for the materials stem from the fact that TCOs are widely used in many different fields of the semiconductor industry such as solar cells, flat-panel displays or liquid crystal devices [11] and, for many of these applications, the patterning of the TCO is necessary. Over the last decade, laser patterning has taken over chemical etching due to it being contact-free, with added flexibility and more environmentally friendly [12,13]. Thus, we believe the proposed model is an interesting tool for the study of laser-scribing processes.

The paper is organized as follows: in Section 2, the proposed method is presented; in section 3 the relevant properties of the two TCOs used in this work, the description of the laser set up and the characterization techniques are described; finally section 4 contains the experimental results gathered and an appropriate discussion while the conclusions are compiled in Section 5.

2. Proposed model

For the interaction between laser pulses and semiconductor materials, such as TCOs, it is generally accepted to refer to Lambert-Beer's law of radiation absorption [14]. This law assumes that the interaction process and the subsequent film ablation are dominated by the absorption of photons with energy above band gap, with little to no contribution from heat transport processes. Under these circumstances, the maximum ablated depth, d_{abl}, obtained when

* Corresponding author at: Centro Láser, Universidad Politécnica de Madrid, Alan Turing 1, Madrid 28031, Spain.
** Corresponding author.
E-mail addresses: david.canteli@upm.es (D. Canteli), ignacio.torres@ciemat.es (I. Torres).

http://dx.doi.org/10.1016/j.apsusc.2017.04.140
0169-4332/

one or several laser pulses hit the surface of a test sample can be expressed as [15]:

$$d_{abl} = N \cdot l_{eff}(N) \cdot \ln\left(\frac{\phi_0}{\phi_{th}(N)}\right) \quad (1)$$

In Eq. (1), N is the number of shots used, ϕ_0 is the peak laser fluence, l_{eff} is the effective penetration depth of the incident light and ϕ_{th} is the material ablation fluence threshold, which in this work refers to the minimum fluence that can produce a visible ablation in the material. The term *ablation fluence threshold,* in its original definition, referred to the energy fluence required to induce phase transformation in a crystal surface [16], but the use of this term has been extended to other meanings, including the one used here.

The material may experience changes in the values of l_{eff} and ϕ_{th} when pulses repeatedly hit the same area, a process known as *incubation*. This process is usually ascribed to a defect creation mechanism [15–19] which generally causes ϕ_{th} to decrease. In the case that incubation is not observed, $l_{eff}(N)$ and $\phi_{th}(N)$ in expression (1) would have to be substituted by l_{eff} and ϕ_{th} [18,20]. The values $l_{eff}(N)$ and $\phi_{th}(N)$ or (l_{eff} and ϕ_{th}) can be obtained by fitting a plot d_{abl} *vs* Log ϕ_0 to Eq. (1) and extracting them from the slope (l_{eff}) and from the intercept with the abscissa(ϕ_{th}). Once both values are known, the ablated depth for single or multiple pulses at any fluence value within or near the studied range can be predicted using Eq. (1).

In addition to hole-drilling, many technological processes involve making a scribe by scanning a laser beam across a workpiece surface. In this case, the ablated depth cannot be predicted solely using Eq. (1), since each pulse that affects a particular point P in the surface is going to do so with a different energy. Fig. 1 aims to illustrate this situation. If we focus onto an arbitrary point P in the surface and consider only the case of Gaussian pulses with a fluence distribution $\phi(r) = \phi_0 \cdot \exp^{-2r^2/\omega_0{}^2}$, it is easy to see that the total energy that reaches point P can be expressed as:

$$\phi_{total} = \phi_0 \cdot \left[1 + \exp^{-2d^2/\omega_0^2} + \exp^{-2(-d)^2/\omega_0^2} + \exp^{-2(2d)^2/\omega_0^2} + \exp^{-2(-2d)^2/\omega_0^2} + \cdots\right] = \phi_0 \cdot \left[1 + 2\sum_{n=1}^{\infty} \exp^{-\frac{2n^2d^2}{\omega_0^2}}\right] \quad (2)$$

Where f is the repetition frequency for the laser, v is the scanning speed, $d = v/f$, is the distance between two consecutive pulses and ω_0 is the spot radius. Conveniently, if we define the overlap between adjacent pulses as $s = 100\cdot(1 - d\,(/2\omega_0))$ it can be shown that for $s > 60\%$ Eq. (2) converges very rapidly to $\sqrt{8/\pi} \cdot E_P \cdot f/(2\omega_0 \cdot v)$, which is the expression for the total fluence reaching point P in the case of a continuous wave Gaussian beam (with $E_p \cdot f$ replaced by the average laser power).

As mentioned earlier, of all the pulses considered in (2) only those that put up an energy above ϕ_{th} can contribute to the visible ablation of the material. As an example in the sketch depicted in Fig. 1 just the three shaded pulses would contribute to the ablation of material at point P. If we now combine Eqs. (1) and (2), it is possible to calculate the ablated depth of a train of pulses by simply adding the contributing terms of the following expression:

$$d_{total} = l_{eff} \cdot \left[\ln\left(\frac{\phi_0}{\phi_{th}}\right) + 2 \cdot \ln\left(\frac{\phi_0 \cdot \exp^{-2d^2/\omega_0^2}}{\phi_{th}}\right) + 2 \cdot \ln\left(\frac{\phi_0 \cdot \exp^{-2(2d)^2/\omega_0^2}}{\phi_{th}}\right) + 2 \cdot \ln\left(\frac{\phi_0 \cdot \exp^{-2(3d)^2/\omega_0^2}}{\phi_{th}}\right) + \cdots\right] \quad (3)$$

i.e., only adding the pulses that fulfill the condition $\phi_0 \cdot \exp^{-2n^2d^2/\omega_0{}^2} \geq \phi_{th}$.

Implicit in Eq. (3) are two conditions that would need to be corroborated before its application. First, the incubation in the material is negligible or very small so that l_{eff} and ϕ_{th} can be considered constant throughout the process. Otherwise, Eq. (3) would simply provide a lower limit to d_{total}. And second, the relationship between ablated material and fluence expressed in Eq. (1) can be used outside the center of the pulse. In other words, the depth achieved anywhere within a crater corresponds with a point where the fluence is ϕ_{th}. In that scenario it is possible to replace ϕ_0 by $\phi_0 \cdot \exp(-2r^2/\omega_0{}^2)$ in Eq. (1) to obtain the ablation depth at any distance (r) from the center of the pulse. If both conditions are fulfilled and the effects associated to radial heat transport remain negligible during the process, then according to Eq. (3) measuring l_{eff} and ϕ_{th} is enough to predict the ablated depth of a scribe given a set of process parameters (v, f, ω_0 and ϕ_0). Lastly, it is important that the geometry of the ablated region does not change considerably, i.e. grooves with a high aspect ratio, so that the fluence does not decrease considerably due to the increase in the effective area.

3. Materials and methods

Films of ITO and AZO were deposited onto 10cm × 10 cm Corning glass 7059 by RF magnetron sputtering (MVSystem). The thickness, sheet resistivity and band-gap were 1400 nm, 3 Ω/sq and 3.75 eV for the ITO films and 650 nm, 3 Ω/sq and 3.65 eV for the AZO films. The holes and the scribes were completed using a diode-pumped solid-state laser (Nd:YVO_4) from Spectra Physics (HIPPO 1064-17 DPSS) with a 1064 nm fundamental frequency tripled to 355 nm. The laser repetition frequency was fixed at 50 kHz throughout all the experiments and the emitted pulses had a Gaussian intensity distribution and pulse duration of 12 ns. The $1/e^2$ beam diameter at focus position, estimated by the method described by Liu in [1] was ~35 μm. Lastly, the laser beam was focused onto the surface of the samples using a scanner (ScanLab HurryScan II 14) with a 250 mm focal length lens, which allowed for process velocities up to 10 m/s. The morphological characterization of the irradiated surfaces, including depth and geometry of the obtained holes and scribes, was made with a confocal microscope (Sensofar PL μ2300).

4. Results and discussion

As stated in Section 2, Eq. (3) is valid only when the material does not show any incubation and the relation between ablation and fluence holds true anywhere within the created crater. Therefore, before assessing the validity of Eq. (3) as a predicting tool for the ablation depth in laser scribing processes both conditions need to be corroborated.

4.1. Incubation under several laser pulses

To check wether the ITO and AZO films showed any incubation, we measured the ablated depth achieved for increasing values of N and ϕ_0. The data obtained for the ITO films can be seen in Fig. 2 represented as *ablated depth* vs *number of shots* for the different values of ϕ_0 tested. A similar plot is obtained for the AZO films (not shown).

Alternatively, in Fig. 3A we have plotted the ablation rate extracted from the slopes of the different data sets of Fig. 2 as a function of fluence. A fit of this data to Eq. (1) results in values of $\phi_{th} = 0.42\,J/cm^2$ and $l_{eff} = 66.5$ nm for the ITO films and of $\phi_{th} = 0.33\,J/cm^2$ and $l_{eff} = 118.0$ nm for the AZO films.

It is clear from the data displayed in Fig. 2 that d_{abl} increases linearly with N as predicted by Eq. (1) meaning that incubation, if present, must be very small. Nevertheless, the scope of incubation

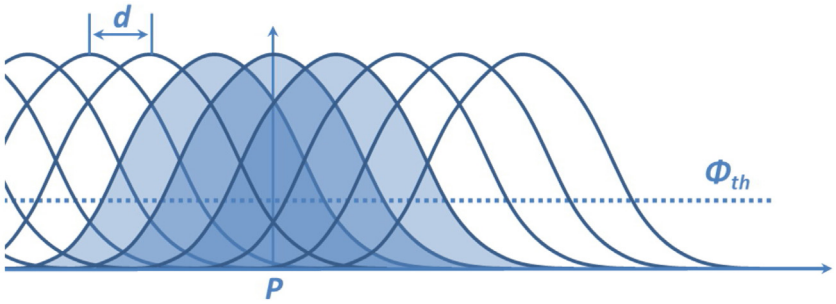

Fig. 1. Schematic representation of a train of Gaussian pulses. Focusing onto an arbitrary point P, only the shadowed pulses, contributing with a fluence higher than ϕ_{th}, would contribute to the net ablation process.

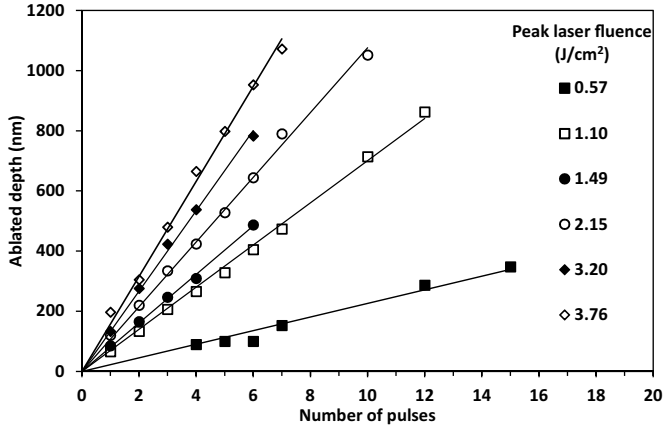

Fig. 2. Ablated depth in ITO films as a function of the incident shot number N for different peak laser fluence values ϕ_0. Solid lines are the linear least-squares fit from which the ablation rate is obtained. A similar plot is obtained for the AZO films.

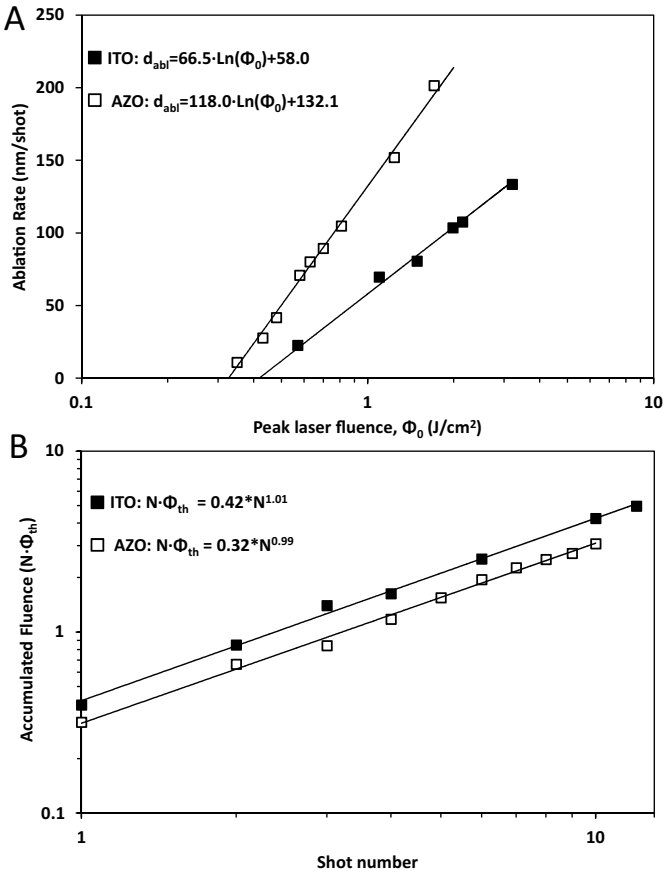

Fig. 3. A: Ablation rate for ITO and AZO films as a function of peak laser fluence. The solid lines represent the least-squares fit according to Eq. (1) and it is used to extract leff (from the slope) and ϕ_{th} (from the intercept with the abscissa). B: Accumulation curve for ITO and AZO films. The solid line represents the least-squares fit to Eq. (4) and it is used to extract the incubation coefficient.

is generally weighed by measuring $\phi_{th}(N)$ at different N values and fitting the results to the following expression [18]:

$$\phi_{th}(N) = \phi_{th}(1) \cdot N^{\zeta-1} \tag{4}$$

In expression (4), appropriate for both metals [15,21] and semiconductors [22], the extent of the incubation is determined by the incubation coefficient ζ ($1 \leq \zeta$), with the limit value $\zeta = 1$ standing for the case of no incubation. By fitting the data gathered for the ITO and AZO films to Eq. (4) (see Fig. 3B) we obtained $\zeta \approx 1$ for both materials (as well as ϕ_{th} values that match those obtained from Fig. 3a), showing that up to 11 shots incubation does not play any role in the ablation of both films. It is unclear whether incubation could develop for a much higher number of shots, but the relatively low value of ϕ_{th} coupled with the film's low thicknesses precluded us from exploring that possibility.

4.2. Ablation homogeneity in the irradiated area

To check whether the relationship between ablation depth and fluence holds true anywhere within the crater we could measure the depth across the spot profile from confocal images and compare it to values obtained from Eq. (1) (with ϕ_0 replaced by $\phi(r) = \phi_0 \cdot \exp^{-2r^2/\omega_0^2}$). However, since the profiles were not perfectly smooth, to integrate these irregularities we decided to instead compare the ablated volumes extracted from confocal images (see diamonds in Fig. 4) to values calculated assuming that the measured values of l_{eff} and ϕ_{th} remain constant throughout the crater. To calculate those volumes, we assumed that the shape of a crater left by a Gaussian pulse is similar to that of a paraboloid of revolution (as observed in confocal images), i.e.:

$$V = \left(\frac{D^2\pi}{4}\right) \cdot \frac{d_{abl}}{2} \tag{5}$$

Where D is the crater diameter. Writing D as a function of ϕ_{th} as:

$$D^2 = 2\omega_0^2 \cdot \ln\left(\frac{\phi_0}{\phi_{th}}\right) \tag{6}$$

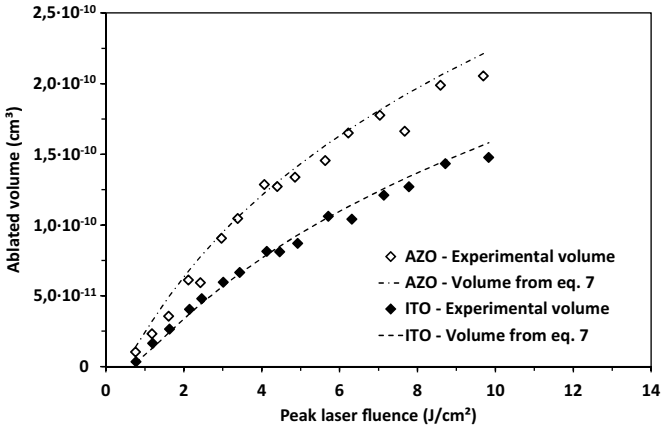

Fig. 4. Comparison between experimental measurements and calculations of the ablated volume of craters obtained from single laser pulses.

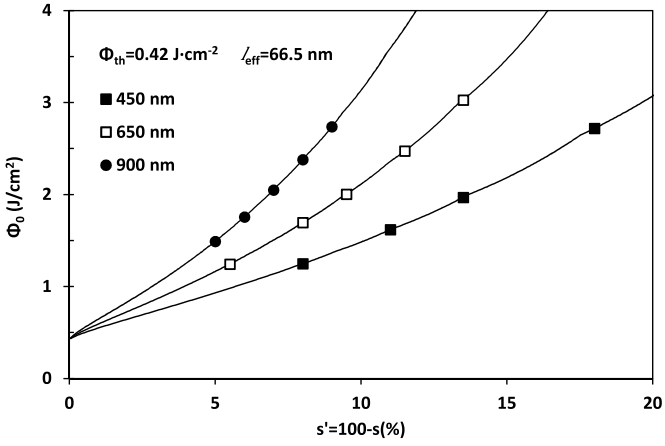

Fig. 5. Process parameters to generate scribes with 450 nm, 650 nm and 900 nm depth calculated using Eq. (3) and the values of l_{eff} and ϕ_{th} obtained in paragraph 4.1 (solid lines). The highlighted symbols are the process parameters chosen to generate the experimental scribes.

and substituting d_{abl} by Eq. (1) (with $N = 1$) it is possible to rewrite Eq. (5) as follows:

$$V = \frac{\pi l_{eff}\omega_0^2}{4}\ln^2\left(\frac{\Phi_0}{\Phi_{th}}\right) \quad (7)$$

The volumes calculated using Eq. (7) with the values of l_{eff} and ϕ_{th} extracted from Fig. 3 are represented by dotted lines in Fig. 4. As can be seen, the calculations match satisfactorily the experimental values, supporting the use of Eq. (1) outside of the crater's center.

4.3. Model deployment and scribes depth

Paragraphs 4.1 and 4.2 showed that the conditions leading to the formulation of expression (3) are met for both the ITO and AZO samples. In order to check the validity of Eq. (3) we have used two different approaches for ITO and AZO.

For ITO we computed the process parameters necessaries to obtain grooves 450 nm, 650 nm and 900 nm deep using the values of l_{eff} and ϕ_{th} obtained in sub-section 4.1. The results of this calculation can be seen as solid lines in Fig. 5. We then chose different conditions to generate the grooves and measure their depths, which are the highlighted points in Fig. 5.

Fig. 5 displays the data as a function of the parameter $s' = 100\text{-}s(\%) = v/f{\cdot}D$ simply for convenience, although it also provides some extra visual information. As mentioned in section 2, the total fluence reaching a point in the material surface can be expressed as $\Phi_{total} = \sqrt{\pi/8}\cdot E_p f/(2\omega_0 v) = \sqrt{\pi/8}\cdot\Phi_0/s'$. Therefore, it is easy to see that any set of conditions that fall in a straight line crossing the origin would have the same ϕ_{total}, which is not the case here since ϕ_{total} does not dictate the depth of the scribes as discussed in Section 2.

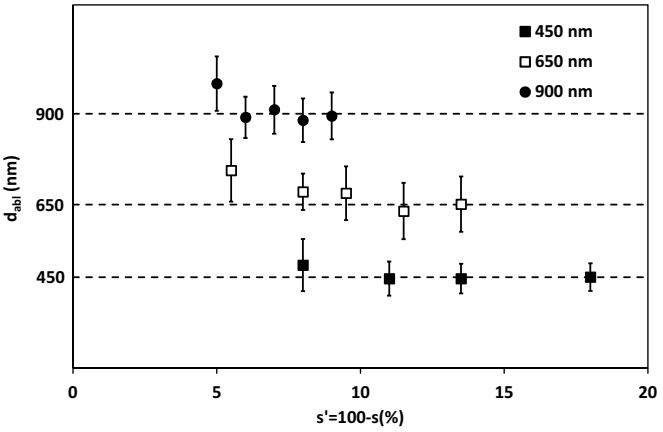

Fig. 6. Average depth of the grooves in ITO obtained with the overlap and fluence parameters selected in Fig. 5. The error-bars shown are the σ_{rms} measured at the bottom of the grooves.

After making the scribes, their respective mean depths were measured from confocal images by averaging the value along several hundred micrometers. The grooves showed a smooth profile with a relatively flat bottom. According to the σ_{rms} value supplied by the confocal own imaging software, the mean depth had a deviation that never surpassed a 12% threshold. The values measured can be seen in Fig. 6, where the error bars are given by the σ_{rms} observed. The grooves had a mean depth that was very near the expected values in most cases. Only the two grooves made using the highest overlap tested (~95%) showed some larger deviations.

We do not have a clear explanation for the deviation in the grooves depth observed at high overlaps. One possible explanation could be the apparition of incubation at the highest overlap values. In our incubation study we only went up to 11 pulses, but at overlap values between 5 and 10%, the number of pulses contributing with fluence above ϕ_{th} are about 10–20 pulses. Therefore, we cannot rule out the apparition of incubation, in which case Eq. (3) would just give a minimum value for the experimental depth.

In the case of the AZO films, the combination of a lower thickness and a lower ϕ_{th} means that the previous approach is more difficult to carry out. Instead, we focused on the complete elimination of the film. We performed a series of laser grooves with different overlap and peak fluence values and grouped the results in Fig. 7 according to the depth obtained: the white diamonds correspond with scribes that did not reach the substrate; the black triangles with those where the glass substrate was exposed albeit only in part of the groove; and the white circles those that reached the substrate all throughout. We then computed the parameters needed to obtain scribes 650 nm deep according to Eq. (3) with the values of ϕ_{th} and l_{eff} given in paragraph 4.1 and added the results to Fig. 7 as the dotted line. Similar to ITO, the computed results match rather well with the experimental results and the dotted line never deviates from the region delimited by black triangles.

At the lowest overlap values, the computed results correlate rather well with the minimum fluence needed to expose the substrate in at least part of the scribe. However, as the overlap increases, the dotted line deviates from that boundary towards higher fluence values. This behavior is similar to what was observed

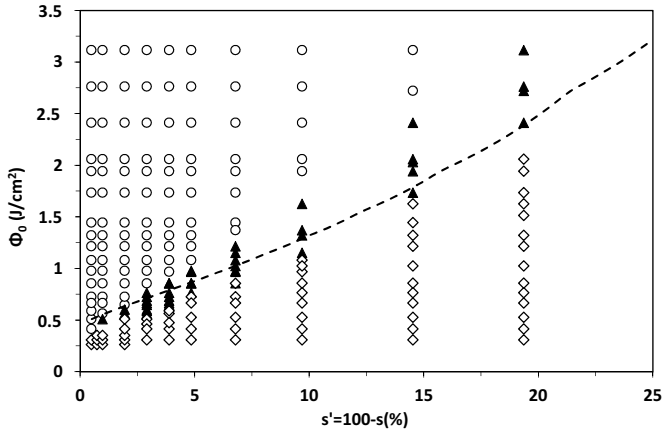

Fig. 7. Collection of parameters used to perform scribes in the AZO films. White diamonds represent scribes that did not reach the glass substrate; black triangles correspond to scribes that reached the substrate but not continuously; and white circles correspond to scribes that reached the substrate in its full length. The dotted line represents the set of parameters obtained when using Eq. (3) for d_{total} 650 nm, with ϕ_{th} = 0.33 J/cm² and l_{eff} = 118.0 nm.

in ITO and therefore a similar explanation in terms of incubation appearing at overlap values above 90% can be proposed.

So, despite the larger departure between computed and experimental results at high overlaps, we believe the correlation for both materials is very good. If the conditions of no incubation and ablation homogeneity are fulfilled, Eq. (3) seems to provide a very good approximation for the depth achieved without the need to implement more complex models, making it a convenient first approach to study laser scribing processes. Future plans include trying out different materials and different laser sources and temporal regimes to further validate the model.

5. Conclusions

We have presented a very simple model that can be used to predict the depth of a groove in laser scribing processes. This simple model is in contrast with the various models available in the literature for its simplicity and ease of use since only process parameters and easy to measure material properties like the effective penetration depth of the incident light, l_{eff}, and the material ablation fluence threshold, ϕ_{th}, are needed. The expression was developed for the case where two conditions are met i.e., the material does not show any incubation and the ablated depth at any point within the crater depends only on the material and on the received fluence at that point.

The expression was tested with nanosecond laser pulses at 355 nm in ITO and AZO films. For both materials, we measured experimentally the values for ϕ_{th} and l_{eff} and also made sure that the above conditions were met in at least a significant range. We then show how the proposed expression matches very accurately the experimental results for both ITO and AZO films over a significant range of pulse overlap and pulse peak fluence values. Only for the highest pulse overlap values used does the computed and experimental results deviates slightly from each other. This behavior could be due to the appearance of incubation in the films, since at overlap values above 90% the number of pulses contributing with fluence above ϕ_{th} are above the maximum number of pulses we used in the incubation study. Nevertheless, the obtained results show that this simple model can provide accurate results when predicting the depth in laser scribing process.

Acknowledgements

Partial financial support for this work has been provided by the Spanish Ministry of Science and Innovation under the projects AMIC (ENE2010-21384-C04-01/04), INNDISOL (IPT-420000-2010-6) and HELLO (ENE2013-48629-C4-3-R, ENE2013-48629-C4-4-R). The authors would like to thank Dr. S. Fernández for the deposition of the ITO and AZO films and her help in the films characterization.

Bibliography

[1] H.W. Choi, D.F. Farson, J. Bovatsek, A. Arai, D. Ashkenasi, Direct-write patterning of indium-tin-oxide film by high pulse repetition frequency femtosecond laser ablation, Appl. Opt. 46 (2007) 5792–5799.
[2] C.C. Mai, J. Lin, An investigation of the surface contours in laser grooving, Int. J. Adv. Manuf. Technol. 28 (1–2) (2006) 76–81.
[3] K. Farooq, A. Kar, Removal of laser-melted material with an assist gas, J. Appl. Phys. 83 (1998) 7467–7473.
[4] A.A. Cenna, P. Mathew, Analysis and prediction of laser cutting parameters of fibre reinforced plastics (FRP) composite materials, Int. J. Mach. Tools Manuf. 42 (1) (2002) 105–113.
[5] C.T. Pan, H. Hocheng, The anisotropic heat-affected zone in the laser grooving of fiber-reinforced composite material, J. Mater. Process. Technol. 62 (1–3) (1996) 54–60.
[6] P. Sheng, G. Chryssolouris, Theoretical model of laser grooving for composite materials, J. Compos. Mater. 29 (1) (1995) 96–112.
[7] P. Solana, P. Kapadia, J. Dowden, A mathematical analysis of heating effects and electrode erosion in conical electrical arc cathodes, J. Phys. D: Appl. Phys. 31 (1998) 3446–3456.
[8] S. Tosto, Modeling and computer simulation of pulsed-laser-induced ablation, Appl. Phys. A Mater. Sci. Process. 68 (4) (1999) 439–446.
[9] A. Stournaras, K. Salonitis, P. Stavropoulos, G. Chryssolouris, Theoretical and experimental investigation of pulsed laser grooving process, Int. J. Adv. Manuf. Technol. 44 (1–2) (2009) 114–124.
[10] P. Parandoush, A. Hossain, A review of modeling and simulation of laser beam machining, Int. J. Mach. Tools Manuf. 85 (2014) 135–145.
[11] C.G. Granqvist, Transparent conductors as solar energy materials: a panoramic review, Sol. Energy Mater. Sol. Cells 91 (17) (2007) 1529–1598.
[12] W.T. Hsiao, S.F. Tseng, K.C. Huang, D. Chiang, Electrode patterning and annealing processes of aluminum-doped zinc oxide thin films using a UV laser system, Opt. Lasers Eng. 51 (1) (2013) 15–22.
[13] S.F. Tseng, W.T. Hsiao, K.C. Huang, D. Chiang, M.F. Chen, C.P. Chou, Laser scribing of indium tin oxide (ITO) thin films deposited on various substrates for touch panels, Appl. Surf. Sci. 257 (5) (2010) 1487–1494.
[14] D. Bäuerle, Laser Processing and Chemistry, Springer, 2011.
[15] P. Mannion, J. Magee, E. Coyne, G.M. O'Connor, T.J. Glynn, The effect of damage accumulation behaviour on ablation thresholds and damage morphology in ultrafast laser micro-machining of common metals in air, Appl. Surf. Sci. 233 (2004) 275–287.
[16] J.M. Liu, Simple technique for measurements of pulsed Gaussian-beam spot sizes, Opt. Lett. 7 (1982) 196–198.
[17] G.B. Blanchet, P. Cotts, C.R. Fincher, Incubation: subthreshold ablation of poly-(methyl methacrylate) and the nature of the decomposition pathways, J. Appl. Phys. 88 (5) (2000) (p. 2975).
[18] Y. Jee, M.F. Becker, R.M. Walser, Laser-induced damage on single-crystal metal surfaces, J. Opt. Soc. Am. B 5 (1988) 648–659.
[19] D. Ashkenasi, M. Lorenz, R. Stoian, A. Rosenfeld, Surface damage threshold and structuring of dielectrics using femtosecond laser pulses: the role of incubation, Appl. Surf. Sci. 150 (1999) 101–106.
[20] J. Ihlemann, J. Meinertz, G. Danev, Excimer laser ablation of thick SiOx-films: etch rate measurements and simulation of the ablation threshold, Appl. Phys. Lett. 101 (9) (2012) 91901–91904.
[21] J. Byskov-Nielsen, J.-M. Savolainen, M. Christensen, P. Balling, Ultra-short pulse laser ablation of metals: threshold fluence, incubation coefficient and ablation rates, Appl. Phys. A Mater. Sci. Process. 101 (1) (2010) 97–101.
[22] J. Bonse, J.M. Wrobel, J. Krüger, W. Kautek, Ultrashort-pulse laser ablation of indium phosphide in air, Appl. Phys. A Mater. Sci. Process. 72 (2001) 89–94.